



Bilateral Synchronization of Hippocampal Early Sharp Waves in Neonatal Rats

Guzel Valeeva^{1†}, Azat Nasretidinov^{1†}, Veronika Rychkova¹ and Roustem Khazipov^{1,2}

¹Laboratory of Neurobiology, Kazan Federal University, Kazan, Russia, ²Aix-Marseille University, INMED, Institut National de la Santé et de la Recherche Médicale (INSERM), Marseille, France

In the neonatal rodent hippocampus, the first and predominant pattern of correlated neuronal network activity is early sharp waves (eSPWs). Whether and how eSPWs are organized bilaterally remains unknown. Here, using simultaneous silicone probe recordings from the left and right hippocampus in neonatal rats *in vivo* we found that eSPWs are highly synchronized bilaterally with nearly zero time lag between the two sides. The amplitudes of eSPWs in the left and right hippocampi were also highly correlated. eSPWs also supported bilateral synchronization of multiple unit activity (MUA). We suggest that bilateral correlated activity supported by synchronized eSPWs participates in the formation of bilateral connections in the hippocampal system.

OPEN ACCESS

Edited by:

Enrico Cherubini,
Scuola Internazionale Superiore di
Studi Avanzati (SISSA), Italy

Reviewed by:

Hajime Hirase,
RIKEN Brain Science Institute (BSI),
Japan
Daniele Linaro,
VIB & KU Leuven Center for Brain &
Disease Research, Belgium

*Correspondence:

Guzel Valeeva
gurvaleeva@kpfu.ru

[†]These authors have contributed
equally to this work

Received: 04 December 2018

Accepted: 22 January 2019

Published: 07 February 2019

Citation:

Valeeva G, Nasretidinov A,
Rychkova V and Khazipov R
(2019) Bilateral Synchronization of
Hippocampal Early Sharp Waves in
Neonatal Rats.
Front. Cell. Neurosci. 13:29.
doi: 10.3389/fncel.2019.00029

Keywords: hippocampus, neonate, sharp waves, bilateral, synchronization

INTRODUCTION

Interhemispheric synchronization is a hallmark of neuronal network activity in the hippocampal system. Bilateral recordings revealed high level of synchronization of various hippocampal activity patterns including theta and gamma oscillations, sharp waves (SPWs) and paroxysmal activity patterns (Suzuki and Smith, 1987; Buzsáki, 1989, 2015; Buzsáki et al., 2003; Carr et al., 2012; Shinohara et al., 2013; Wang et al., 2014; Pfeiffer and Foster, 2015; Benito et al., 2016; Tanaka et al., 2017; Villalobos et al., 2017). Interhippocampal synchronization is supported by several mechanisms including commissural connections between hippocampi and synchronous input from entorhinal cortex (Mizuseki et al., 2009; Shinohara et al., 2012; Benito et al., 2016; Fernández-Ruiz et al., 2017). However, when and how bilateral synchronization emerges in the hippocampal system remains unknown.

During development, neuronal networks generate particular patterns of correlated activity that participate in the formation of neuronal circuits (Katz and Shatz, 1996; Khazipov and Luhmann, 2006; Blankenship and Feller, 2010; Hanganu-Opatz, 2010; Colonnese and Khazipov, 2012; Luhmann and Khazipov, 2018). Early activity patterns are expressed in a way of local (patchy) intermittent activity bursts such as spontaneous movement driven spindle- and gamma-bursts in somatosensory cortex (Khazipov et al., 2004; Yang et al., 2009, 2013; Mohns and Blumberg, 2010; Minlebaev et al., 2011; Akhmetshina et al., 2016) or retina/cochlea driven waves in visual and auditory cortex, respectively (Hanganu et al., 2006, 2007; Colonnese and Khazipov, 2010; Ackman et al., 2012; Babola et al., 2018). These early forms of neocortical activity occur largely asynchronously in the two hemispheres, however. Lateralization is particularly prominent in somatosensory cortex (Yang et al., 2009; Marcano-Reik et al., 2010). It is also present in visual system where only a small proportion of events, presumably generated by retinal waves originating from binocular retina regions is bilaterally

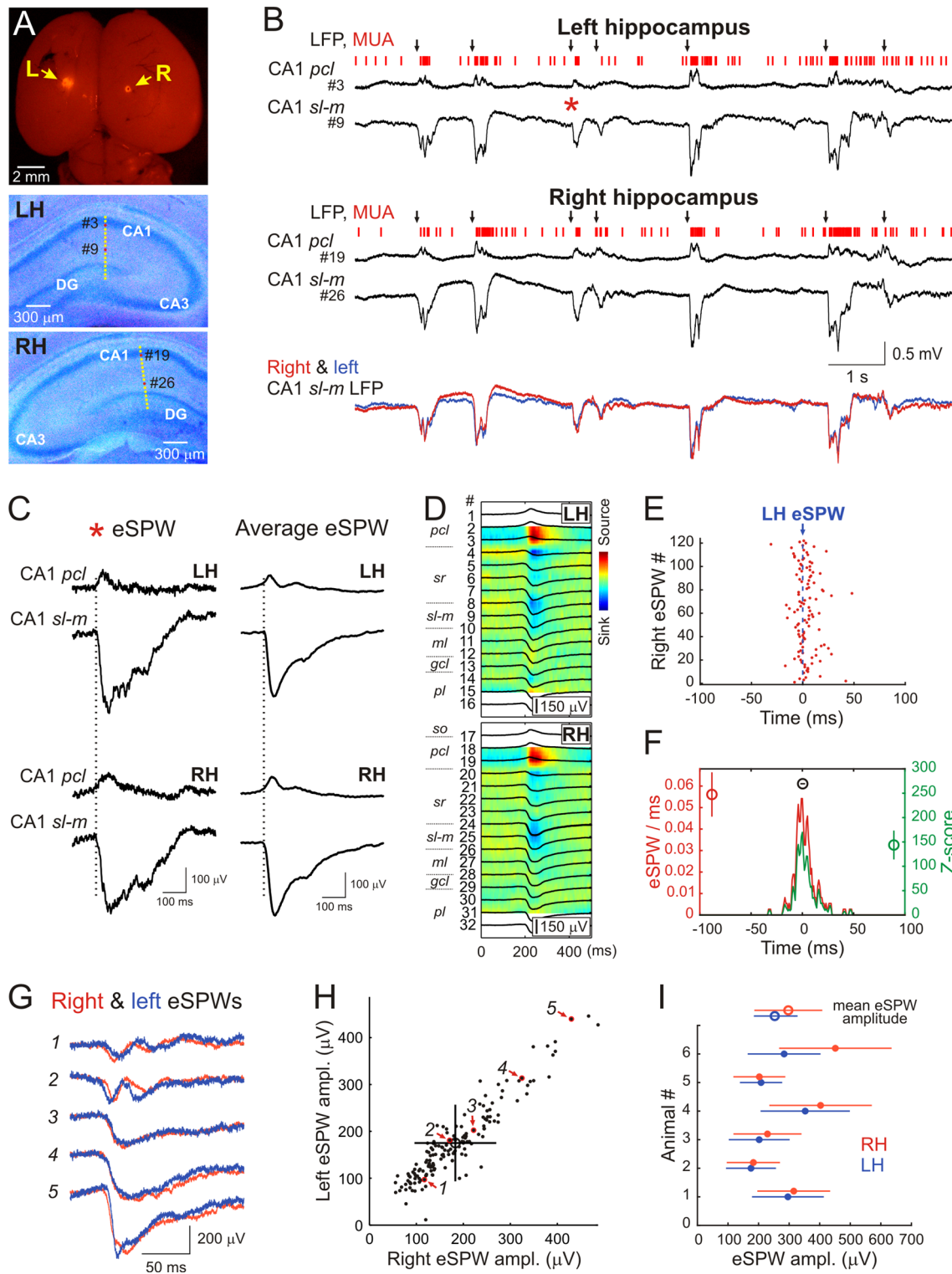


FIGURE 1 | Interhemispheric synchronization of hippocampal early sharp waves (eSPWs) in neonatal rats. **(A)** Top: the microphotograph of Dil traces at insertion sites of two silicone probes on the surface of the left (L) and right (R) brain hemispheres in a P6 rat pup. Middle–Bottom: recording sites of 16-channel probes overlaid on cresyl violet stained coronal slices of the left (LH, middle) and right (RH, bottom) hippocampi. **(B)** Simultaneous local field potential (LFP) and multiple unit activity (MUA) recordings from the left hippocampus and right hippocampi from CA1 pyramidal cell layer (*pcl*, recording sites #3 and #19 on panel A) and strata lacunosum-moleculare (*sl-m*, recording sites #9 and #26 on panel A). Black arrows above the traces indicate eSPWs. Bottom, overlaid *sl-m* LFP traces from left (blue) and right (red) hippocampi. (Continued)

FIGURE 1 | Continued
 and right (red) hippocampus. **(C)** The eSPW from panel **(B)**; red asterisk and average left eSPW-triggered LFP in the left and right hippocampus on expanded time scale. **(D)** Left eSPWs-triggered LFPs (black) in the left and right hippocampi overlaid on CSD maps. **(E)** Left eSPW onset-triggered raster plot of right eSPW onsets. **(F)** Left eSPW onset-triggered normalized PETH of right eSPW onsets (red) and corresponding z-score values (green). Group averages (mean \pm SD; $n = 6$ animals) show the peak value of normalized PETH (red circle), the peak value of z-score (green circle) and the time lag between left and right eSPWs (black circle). **(G)** Five example traces of eSPWs recorded simultaneously in CA1 *sl-m* of left (blue) and right (red) hippocampi. **(H)** Relationships between left and right eSPW amplitudes recorded in CA1 *sl-m* layer (animal #2). Average amplitude values are indicated by an open circle with error bars corresponding to SD. Red arrows indicate the data points (outlined with red) corresponding to eSPWs shown on panel **(G)**. See also **Supplementary Figure S1** for all animals. **(I)** Amplitude averages of eSPWs in the left (blue) and right (red) hippocampi of six P5–7 rats (closed circles) and group values (open circles). Error bars show SD.

synchronized (Hanganu et al., 2006; Ackman et al., 2012), and in the auditory system where cochlea driven activities are biased towards predominant contralateral cochlear input (Babola et al., 2018).

In the neonatal hippocampus, the first and predominant pattern of correlated neuronal network activity is early SPWs (eSPWs; Leinekugel et al., 2002; Karlsson et al., 2006; Mohns et al., 2007; Mohns and Blumberg, 2008; Marguet et al., 2015; Valeeva et al., 2019). eSPWs are intermittent events characterized by sharp negative potentials in CA1 strata lacunosum-moleculare (*sl-m*) and radiatum (*sr*) reversing at pyramidal cell layer (*pcl*), and synchronous neuronal firing in CA3, CA1 and dentate gyrus. eSPWs are generated by cooperation of inputs from medial entorhinal cortex and intrinsic intrahippocampal connections. eSPWs are typically triggered by spontaneous myoclonic neonatal movements and are preceded by activity bursts in superficial layers 2–3 of medial entorhinal cortex (Karlsson et al., 2006; Marguet et al., 2015; Valeeva et al., 2019). However, whether eSPWs support bilateral synchronization of activity in the left and right hippocampus as adult SPWs do (Suzuki and Smith, 1987; Buzsáki, 1989, 2015) remains an open question.

Here, we addressed this question by bilateral recordings from the right and left CA1 hippocampus using silicone probes in neonatal P5–7 non-anesthetized head restrained rat pups. We found that nearly all eSPWs occur in both hippocampi synchronously with almost zero time lag and that eSPWs support high level of bilateral synchronization of neuronal activity.

MATERIALS AND METHODS

Ethical Approval

This work has been carried out in accordance with EU Directive 2010/63/EU for animal experiments and all animal-use protocols were approved by the French National Institute of Health and Medical Research (INSERM, protocol N007.08.01) and Kazan Federal University on the use of laboratory animals (ethical approval by the Institutional Animal Care and Use Committee of Kazan State Medical University N9-2013).

Animal Preparation

Wistar rats of either sex from postnatal days (P) 5–7 were used. Preparation of the animals for recordings was performed under deep isoflurane anesthesia the day before recording as previously described (Akhmetshina et al., 2016; Valeeva et al., 2019). Briefly, while under isoflurane anesthesia the skull was cleared of skin and periosteum and covered by dental cement, leaving ≈ 5 mm² windows above the left and right hippocampi. The wound was treated with xylocaine (2%) and chlorhexidine (0.05%). Animals were warmed up and returned to the litter to recover from surgery and did not receive additional medications during recordings.

Electrophysiological Recordings

Recordings were performed from head-restrained non-anesthetized rats. A metal ring was fixed to the skull with dental cement and *via* ball-joint to a magnetic stand. Animals were surrounded by a cotton nest and heated *via* a thermal pad (35–37°C). During recordings, animals were regularly fed with heated milk and continuously monitored for any sign of pain or discomfort, and if such occurred, the animals were sacrificed with an overdose of urethane.

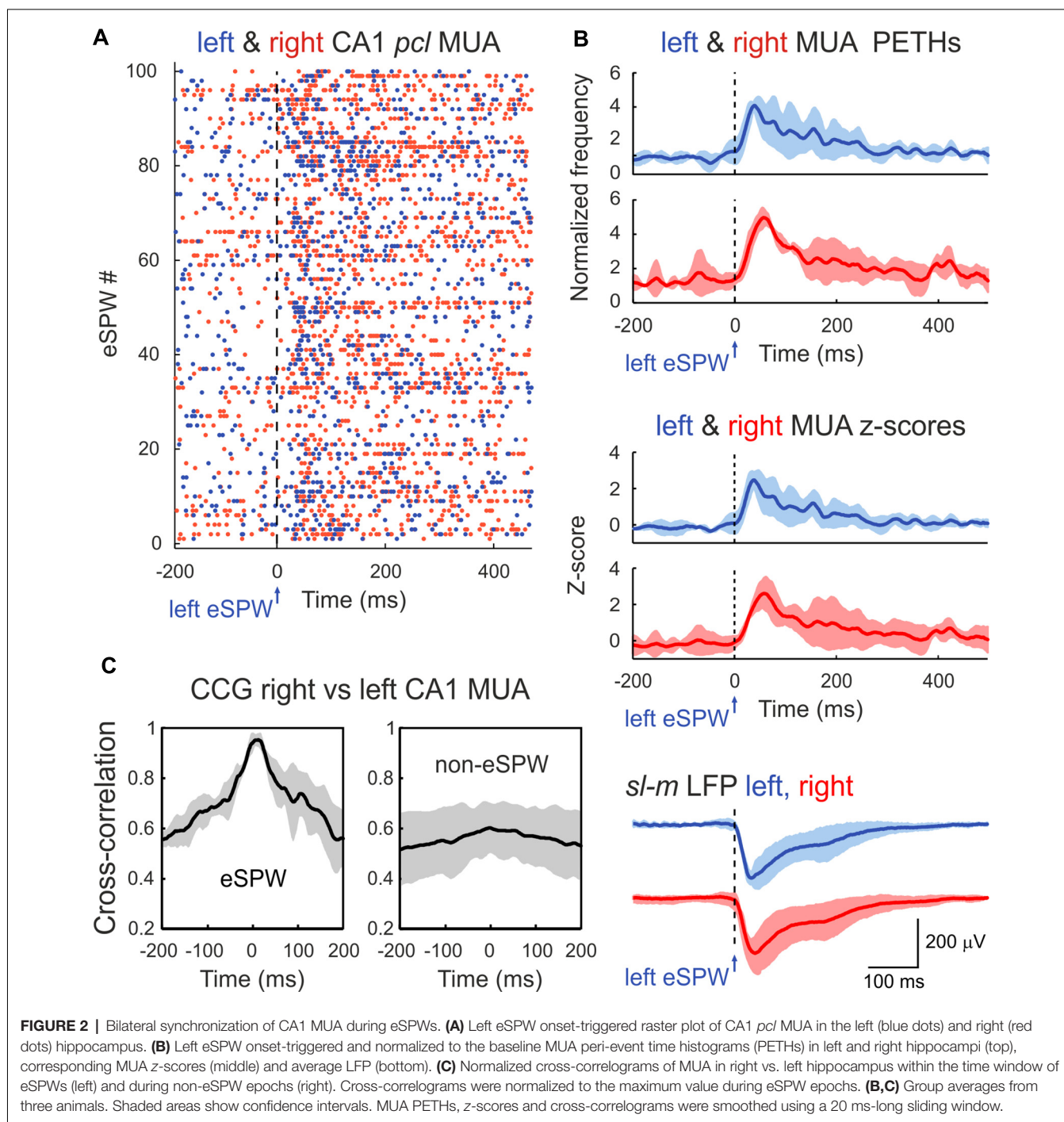
Extracellular recordings of local field potentials (LFPs) and multiple unit activity (MUA) were performed along the CA1–dentate gyrus axis of the dorsal hippocampus using a pair of 16-site linear silicon probes with 50 μ m separation distance between the electrodes (four animals) or two eight-shank 64-site probes with 200 μ m separation distance (two animals; NeuroNexus, Ann Arbor, MI, USA). Two craniotomies of 0.2–0.3 mm diameter each were performed above the left and right hippocampi. DiI coated electrodes were placed using stereotaxic coordinates (Khazipov et al., 2015). A chloride silver wire, placed in the neocortex, served as a ground electrode. Signals from extracellular recordings were amplified and filtered (10,000 \times ; 0.15–10 kHz) using DigitalLynxSX amplifier (Neuralynx, Bozeman, MT, USA) and digitized at 32 kHz. From 30 min to an hour of spontaneous activity were recorded in each animal.

Histology

After recordings the animals were deeply anesthetized with urethane (3 g/kg, intraperitoneally) and perfused intracardially with 4% paraformaldehyde and 1% glutaraldehyde (Sigma). The brains were removed and left for fixation for a few days. One-hundred micron-thick coronal slices were cut using a Vibratome (Thermo Fisher Scientific, Waltham, MA, USA). Electrode positions were identified from the DiI tracks overlaid on the microphotographs of sections after cresyl violet staining.

Data Analysis

Wideband recordings were preprocessed using custom-written functions in MATLAB (MathWorks, Natick, MA, USA). eSPWs were detected semi-automatically from down-sampled (1,000 Hz), bandpass filtered (3–100 Hz, Chebyshev type 2 Filter) LFP signal. All events reaching the amplitude greater than 1.5 standard deviations at filtered LFP on *sl-m* and *pcl* channels (negative and positive peaks, respectively) were first considered



as putative eSPWs. To discard movement and static artifacts, LFP segments from -1 s to 1 around the eSPW were visually inspected. The eSPW onset was defined as a time when the first LFP derivative in *sl-m* reached a threshold of 2 mV/s. Raw data were filtered using 250 – $4,000$ Hz bandpass wavelet filter (Daubechies 4) and spikes were detected as negative events exceeding -3.5 standard deviations of filtered signal. Time lags between the left and right hippocampus were calculated from peri-onset time histograms smoothed by moving average filter

(4 ms window for eSPWs onsets and 20 ms for MUA). Z-scores were estimated on the basis of a shuffled artificial data as described previously (Valeeva et al., 2019).

Statistics

Statistical analysis was performed using the MATLAB Statistics toolbox. Group comparisons were done using one- and paired-sample Wilcoxon signed-rank tests. *P*-value of less than 0.05 was considered significant. Correlations between variables were

estimated using the Pearson (r) correlation coefficients. Unless indicated, data are presented as mean \pm SD.

RESULTS

In the present study we performed simultaneous LFP and MUA recordings from the dorsal part of the left and right CA1 hippocampus in six non-anesthetized head-restrained postnatal days [P] 5–7 rats (Figure 1). The location of the recording sites was identified during *post hoc* analysis of the DiI electrode tracks in coronal sections (Figure 1A).

In keeping with previous results, hippocampal activity on both sides was characterized by the ripple-lacking eSPWs which were associated with a negative sharp potential below the CA1 *sr* and *sl-m* and polarity reversal at the *pcl*, and often followed by “tails” (Leinekugel et al., 2002; Karlsson et al., 2006; Mohns et al., 2007; Mohns and Blumberg, 2008; Marguet et al., 2015; Valeeva et al., 2019; Figures 1B–D). eSPWs attained maximal negativity in *sl-m* (left: $253 \pm 68 \mu\text{V}$; right: $297 \pm 111 \mu\text{V}$; $n = 6$) and their current-source density profile was characterized by the two main sinks, one in *sr* and another in *sl-m* (Figure 1D) as reported previously (Valeeva et al., 2019). eSPWs were also associated with MUA bursts (Figures 1B, 2A–C). The frequencies of eSPWs in the left and right hippocampus were of $3.8 \pm 1.5/\text{min}$ and $3.9 \pm 1.6/\text{min}$, respectively ($p = 0.44$). As shown in Figure 1B, eSPWs in the right and left hippocampus were also highly synchronized. We further assessed the bilateral co-occurrence probability and the time lags between eSPWs in the right and left hippocampi. We found that $97 \pm 4\%$ of eSPWs in the right hippocampus co-occurred with eSPWs in the left hippocampus (z -score = 144 ± 30) and, vice versa, $96 \pm 4\%$ of eSPWs in the left hippocampus co-occurred with eSPWs in the right hippocampus (z -score = 140 ± 29) within a ± 100 ms time window (Figures 1E,F). The vast majority of eSPWs occurred simultaneously with nearly zero time lag between hemispheres, although some eSPWs occurred with a time lag in the range of up to 10 ms. On average, the time lags separating eSPWs in the left and right hippocampi were of 0.3 ± 2.3 ms. These results indicate that eSPWs are highly synchronized bilaterally.

eSPWs in the left and right hippocampi also highly correlated in amplitude. While the eSPWs' amplitude varied in both sides, larger in amplitude eSPWs in one hippocampus were associated with larger eSPWs in the contralateral hippocampus (Figures 1G–I, Pearson's $r = 0.84 \pm 0.14$; $n = 6$; $p < 0.001$; see also Supplementary Figure S1 for all animals). Also, eSPWs were slightly more ample in the right hippocampus ($p = 0.03$).

In agreement with the results from previous studies, eSPWs were associated with an increase in MUA in CA1 *pcl*. MUA peri-event time histograms (PETHs) triggered by left eSPW onsets attained maximal values of 0.04 ± 0.01 spikes/ms (4.2 ± 0.2 -fold increase above baseline; z -score 2.6 ± 0.5) and 0.05 ± 0.02 spikes/ms (5.0 ± 0.4 -fold increase above baseline; z -score 2.6 ± 0.8) with time lags of 41 ± 8 ms and 60 ± 4 ms ($p > 0.05$) in the left and right hippocampi, respectively (Figures 2A,B; $n = 3$ rats; animals with MUA frequency < 5 /s

were excluded from MUA analysis). Co-occurrence of eSPWs in the left and right hippocampi supported bilateral MUA synchronization during eSPWs that was evident on the MUA cross-correlograms within a time window of ± 1 s from the eSPW onset. Peak of MUA cross-correlation during eSPWs attained 0.027 ± 0.014 and showed a time lag of 9 ± 9 ms between the left and right hippocampi. Bilateral MUA cross-correlation was also observed during the non-eSPW epochs, but its level was lower (0.017 ± 0.008 with a time lag of 18 ± 9 ms) than during eSPWs (Figure 2C).

DISCUSSION

Our main finding is that eSPWs are highly synchronized and support correlated neuronal activity in the left and right hippocampus in the rat pups *in vivo*. Previously, several forms of synchronized bilateral activity in the developing hippocampal system have been described *in vitro*. For example, giant depolarizing potentials (GDPs), recurrent neuronal network discharges originating in CA3 network are synchronized bilaterally in the preparation of interconnected hippocampi *in vitro* (Khalilov et al., 1997; Leinekugel et al., 1998). Epileptiform discharges induced by various epileptogenic agents also propagate between hippocampi and bilaterally synchronize hippocampal activity in this preparation (Khalilov et al., 1997, 1999, 2005; Khazipov et al., 1999). Lesion of the ventral hippocampal commissure or pharmacological suppression of commissural action potential propagation results in complete bilateral desynchronization of GDPs and paroxysmal activities indicating that commissural communication is pivotal for their bilateral synchronization (Khalilov et al., 1999; Khazipov et al., 1999). Consistent with these findings *in vitro*, we found perfect bilateral synchrony in eSPWs in neonatal rat pups *in vivo*. Bilateral eSPWs synchronization likely involves CA3-CA3 commissural connections as in the case of GDPs and paroxysmal events *in vitro* as described above. This is supported by activation of CA3 neurons during eSPWs also manifested by a current sink of eSPWs in CA1 *sr*, where CA3-CA1 synapses are located (Valeeva et al., 2019). However, bilateral eSPWs synchronization *in vivo* may also involve synchronous bilateral inputs from entorhinal cortex that is evidenced by synchronous eSPWs' current sinks in CA1 *sl-m*, where synapses from the entorhinal cortex are located (*ibid*). This suggests that the activity bursts in superficial layers of entorhinal cortex preceding hippocampal eSPWs are also bilaterally synchronized. In the future, it would be of interest to determine mechanisms involved in bilateral activation of entorhinal cortex in relation to eSPWs and spontaneous body movements, which reliably trigger entorhinal-hippocampal activity in neonatal rats (Karlsson et al., 2006; Marguet et al., 2015; Valeeva et al., 2019).

In conclusion, we have shown that bilateral synchronization of activity in the hippocampal system emerges early during postnatal development and that early bilateral synchronization is supported by highly correlated eSPWs. Bilateral synchronization of eSPWs likely contributes to the development of synaptic connections between hippocampi by means of synchronization

of neuronal activity and activity-dependent plasticity. Our results also provide further evidence that eSPWs are a developmental prototype of adult SPWs, which also display a high level of bilateral synchrony (Suzuki and Smith, 1987; Buzsáki, 1989, 2015).

DATA AVAILABILITY

Original and processed data, and signal processing and analysis routines are available on request from the authors.

AUTHOR CONTRIBUTIONS

RK and GV conceived the project. GV and VR performed the experiments. AN, GV and VR analyzed the data. RK wrote the article.

FUNDING

This work was supported by the subsidy allocated to Kazan Federal University for the state assignment in the sphere of

REFERENCES

- Ackman, J. B., Burbridge, T. J., and Crair, M. C. (2012). Retinal waves coordinate patterned activity throughout the developing visual system. *Nature* 490, 219–225. doi: 10.1038/nature11529
- Akhmetshina, D., Nasretidinov, A., Zakharov, A., Valeeva, G., and Khazipov, R. (2016). The nature of the sensory input to the neonatal rat barrel cortex. *J. Neurosci.* 36, 9922–9932. doi: 10.1523/JNEUROSCI.1781-16.2016
- Babola, T. A., Li, S., Gribizis, A., Lee, B. J., Issa, J. B., Wang, H. C., et al. (2018). Homeostatic control of spontaneous activity in the developing auditory system. *Neuron* 99, 511.e5–524.e5. doi: 10.1016/j.neuron.2018.07.004
- Benito, N., Martín-Vázquez, G., Makarova, J., Makarov, V. A., and Herreras, O. (2016). The right hippocampus leads the bilateral integration of γ -parsed lateralized information. *Elife* 5:e16658. doi: 10.7554/eLife.16658
- Blankenship, A. G., and Feller, M. B. (2010). Mechanisms underlying spontaneous patterned activity in developing neural circuits. *Nat. Rev. Neurosci.* 11, 18–29. doi: 10.1038/nrn2759
- Buzsáki, G. (1989). Two-stage model of memory trace formation: a role for “noisy” brain states. *Neuroscience* 31, 551–570. doi: 10.1016/0306-4522(89)90423-5
- Buzsáki, G. (2015). Hippocampal sharp wave-ripple: a cognitive biomarker for episodic memory and planning. *Hippocampus* 25, 1073–1188. doi: 10.1002/hipo.22488
- Buzsáki, G., Buhl, D. L., Harris, K. D., Csicsvari, J., Czeh, B., and Morozov, A. (2003). Hippocampal network patterns of activity in the mouse. *Neuroscience* 116, 201–211. doi: 10.1016/s0306-4522(02)00669-3
- Carr, M. F., Karlsson, M. P., and Frank, L. M. (2012). Transient slow γ synchrony underlies hippocampal memory replay. *Neuron* 75, 700–713. doi: 10.1016/j.neuron.2012.06.014
- Colonnese, M. T., and Khazipov, R. (2010). “Slow activity transients” in infant rat visual cortex: a spreading synchronous oscillation patterned by retinal waves. *J. Neurosci.* 30, 4325–4337. doi: 10.1523/JNEUROSCI.4995-09.2010
- Colonnese, M. T., and Khazipov, R. (2012). Spontaneous activity in developing sensory circuits: implications for resting state fMRI. *Neuroimage* 62, 2212–2221. doi: 10.1016/j.neuroimage.2012.02.046
- Fernández-Ruiz, A., Oliva, A., Nagy, G. A., Maurer, A. P., Berényi, A., and Buzsáki, G. (2017). Entorhinal-CA3 dual-input control of spike timing in the hippocampus by theta- γ coupling. *Neuron* 93, 1213.e5–1226.e5. doi: 10.1016/j.neuron.2017.02.017
- Hanganu, I. L., Ben-Ari, Y., and Khazipov, R. (2006). Retinal waves trigger spindle bursts in the neonatal rat visual cortex. *J. Neurosci.* 26, 6728–6736. doi: 10.1523/JNEUROSCI.0752-06.2006
- scientific activities (Ministry of Education and Science of the Russian Federation; 6.5364.2017/9.10 to GV), and was performed in the frame of the program of competitive growth of Kazan Federal University and collaborative agreement between the Institut national de la santé et de la recherche médicale and Kazan Federal University (LIA to RK).

ACKNOWLEDGMENTS

We thank Dr. Andrey Rozov for helpful suggestions and comments on the manuscript.

SUPPLEMENTARY MATERIAL

The Supplementary Material for this article can be found online at: <https://www.frontiersin.org/articles/10.3389/fncel.2019.00029/full#supplementary-material>

FIGURE S1 | Relationships between left and right eSPW amplitudes recorded in CA1 *sl-m* of 6 animals. Pearson's *r* values and corresponding *p*-values are shown above the plots.

Hanganu, I. L., Staiger, J. F., Ben-Ari, Y., and Khazipov, R. (2007). Cholinergic modulation of spindle bursts in the neonatal rat visual cortex *in vivo*. *J. Neurosci.* 27, 5694–5705. doi: 10.1523/JNEUROSCI.5233-06.2007

Hanganu-Opatz, I. L. (2010). Between molecules and experience: role of early patterns of coordinated activity for the development of cortical maps and sensory abilities. *Brain Res. Rev.* 64, 160–176. doi: 10.1016/j.brainresrev.2010.03.005

Karlsson, K. A., Mohns, E. J., di Prisco, G. V., and Blumberg, M. S. (2006). On the co-occurrence of startles and hippocampal sharp waves in newborn rats. *Hippocampus* 16, 959–965. doi: 10.1002/hipo.20224

Katz, L. C., and Shatz, C. J. (1996). Synaptic activity and the construction of cortical circuits. *Science* 274, 1133–1138. doi: 10.1126/science.274.5290.1133

Khalilov, I., Dzhalala, V., Medina, I., Leinekugel, X., Melyan, Z., Lamsa, K., et al. (1999). Maturation of kainate-induced epileptiform activities in interconnected intact neonatal limbic structures *in vitro*. *Eur. J. Neurosci.* 11, 3468–3480. doi: 10.1046/j.1460-9568.1999.00768.x

Khalilov, I., Esclapez, M., Medina, I., Aggoun, D., Lamsa, K., Leinekugel, X., et al. (1997). A novel *in vitro* preparation: the intact hippocampal formation. *Neuron* 19, 743–749. doi: 10.1016/s0896-6273(00)80956-3

Khalilov, I., Le Van Quyen, Q., Gozlan, H., and Ben-Ari, Y. (2005). Epileptogenic actions of GABA and fast oscillations in the developing hippocampus. *Neuron* 48, 787–796. doi: 10.1016/j.neuron.2005.09.026

Khazipov, R., Desfreres, L., Khalilov, I., and Ben-Ari, Y. (1999). Three-independent-compartment chamber to study *in vitro* commissural synapses. *J. Neurophysiol.* 81, 921–924. doi: 10.1152/jn.1999.81.2.921

Khazipov, R., and Luhmann, H. J. (2006). Early patterns of electrical activity in the developing cerebral cortex of humans and rodents. *Trends Neurosci.* 29, 414–418. doi: 10.1016/j.tins.2006.05.007

Khazipov, R., Sirota, A., Leinekugel, X., Holmes, G. L., Ben-Ari, Y., and Buzsáki, G. (2004). Early motor activity drives spindle bursts in the developing somatosensory cortex. *Nature* 432, 758–761. doi: 10.1038/nature03132

Khazipov, R., Zaynutdinova, D., Ogievetsky, E., Valeeva, G., Mitrukina, O., Manent, J. B., et al. (2015). Atlas of the postnatal rat brain in stereotaxic coordinates. *Front. Neuroanat.* 9:161. doi: 10.3389/fnana.2015.00161

Leinekugel, X., Khalilov, I., Ben-Ari, Y., and Khazipov, R. (1998). Giant depolarizing potentials: the septal pole of the hippocampus paces the activity of the developing intact septohippocampal complex *in vitro*. *J. Neurosci.* 18, 6349–6357. doi: 10.1523/JNEUROSCI.18-16-06349.1998

Leinekugel, X., Khazipov, R., Cannon, R., Hirase, H., Ben-Ari, Y., and Buzsáki, G. (2002). Correlated bursts of activity in the neonatal hippocampus *in vivo*. *Science* 296, 2049–2052. doi: 10.1126/science.1071111

- Luhmann, H. J., and Khazipov, R. (2018). Neuronal activity patterns in the developing barrel cortex. *Neuroscience* 368, 256–267. doi: 10.1016/j.neuroscience.2017.05.025
- Marcano-Reik, A. J., Prasad, T., Weiner, J. A., and Blumberg, M. S. (2010). An abrupt developmental shift in callosal modulation of sleep-related spindle bursts coincides with the emergence of excitatory-inhibitory balance and a reduction of somatosensory cortical plasticity. *Behav. Neurosci.* 124, 600–611. doi: 10.1037/a0020774
- Marguet, S. L., Le-Schulte, V. T., Merseburg, A., Neu, A., Eichler, R., Jakovcevski, I., et al. (2015). Treatment during a vulnerable developmental period rescues a genetic epilepsy. *Nat. Med.* 21, 1436–1444. doi: 10.1038/nm.3987
- Minlebaev, M., Colonnese, M., Tsitsadze, T., Sirota, A., and Khazipov, R. (2011). Early γ oscillations synchronize developing thalamus and cortex. *Science* 334, 226–229. doi: 10.1126/science.1210574
- Mizuseki, K., Sirota, A., Pastalkova, E., and Buzsaki, G. (2009). Theta oscillations provide temporal windows for local circuit computation in the entorhinal-hippocampal loop. *Neuron* 64, 267–280. doi: 10.1016/j.neuron.2009.08.037
- Mohns, E. J., and Blumberg, M. S. (2008). Synchronous bursts of neuronal activity in the developing hippocampus: modulation by active sleep and association with emerging γ and theta rhythms. *J. Neurosci.* 28, 10134–10144. doi: 10.1523/JNEUROSCI.1967-08.2008
- Mohns, E. J., and Blumberg, M. S. (2010). Neocortical activation of the hippocampus during sleep in infant rats. *J. Neurosci.* 30, 3438–3449. doi: 10.1523/JNEUROSCI.1967-08.2008
- Mohns, E. J., Karlsson, K. A., and Blumberg, M. S. (2007). Developmental emergence of transient and persistent hippocampal events and oscillations and their association with infant seizure susceptibility. *Eur. J. Neurosci.* 26, 2719–2730. doi: 10.1111/j.1460-9568.2007.05928.x
- Pfeiffer, B. E., and Foster, D. J. (2015). PLACE CELLS. Autoassociative dynamics in the generation of sequences of hippocampal place cells. *Science* 349, 180–183. doi: 10.1126/science.aaa9633
- Shinohara, Y., Hosoya, A., and Hirase, H. (2013). Experience enhances γ oscillations and interhemispheric asymmetry in the hippocampus. *Nat. Commun.* 4:1652. doi: 10.1038/ncomms2658
- Shinohara, Y., Hosoya, A., Yahagi, K., Ferecsko, A. S., Yaguchi, K., Sik, A., et al. (2012). Hippocampal CA3 and CA2 have distinct bilateral innervation patterns to CA1 in rodents. *Eur. J. Neurosci.* 35, 702–710. doi: 10.1111/j.1460-9568.2012.07993.x
- Suzuki, S. S., and Smith, G. K. (1987). Spontaneous EEG spikes in the normal hippocampus. I. Behavioral correlates, laminar profiles and bilateral synchrony. *Electroencephalogr. Clin. Neurophysiol.* 67, 348–359. doi: 10.1016/0013-4694(87)90123-4
- Tanaka, M., Wang, X., Mikoshiba, K., Hirase, H., and Shinohara, Y. (2017). Rearing-environment-dependent hippocampal local field potential differences in wild-type and inositol trisphosphate receptor type 2 knockout mice. *J. Physiol.* 595, 6557–6568. doi: 10.1113/jp274573
- Valeeva, G., Janackova, S., Nasretdinov, A., Rychkova, V., Makarov, R., Holmes, G. L., et al. (2019). Emergence of coordinated activity in the developing entorhinal-hippocampal network. *Cereb. Cortex* 29, 906–920. doi: 10.1093/cercor/bhy309
- Villalobos, C., Maldonado, P. E., and Valdes, J. L. (2017). Asynchronous ripple oscillations between left and right hippocampi during slow-wave sleep. *PLoS One* 12:e0171304. doi: 10.1371/journal.pone.0171304
- Wang, Y., Toprani, S., Tang, Y., Vrabec, T., and Durand, D. M. (2014). Mechanism of highly synchronized bilateral hippocampal activity. *Exp. Neurol.* 251, 101–111. doi: 10.1016/j.expneurol.2013.11.014
- Yang, J. W., An, S., Sun, J. J., Reyes-Puerta, V., Kindler, J., Berger, T., et al. (2013). Thalamic network oscillations synchronize ontogenetic columns in the newborn rat barrel cortex. *Cereb. Cortex* 23, 1299–1316. doi: 10.1093/cercor/bhs103
- Yang, J. W., Hanganu-Opatz, I. L., Sun, J. J., and Luhmann, H. J. (2009). Three patterns of oscillatory activity differentially synchronize developing neocortical networks *in vivo*. *J. Neurosci.* 29, 9011–9025. doi: 10.1523/JNEUROSCI.5646-08.2009

Conflict of Interest Statement: The authors declare that the research was conducted in the absence of any commercial or financial relationships that could be construed as a potential conflict of interest.

Copyright © 2019 Valeeva, Nasretdinov, Rychkova and Khazipov. This is an open-access article distributed under the terms of the Creative Commons Attribution License (CC BY). The use, distribution or reproduction in other forums is permitted, provided the original author(s) and the copyright owner(s) are credited and that the original publication in this journal is cited, in accordance with accepted academic practice. No use, distribution or reproduction is permitted which does not comply with these terms.